arXiv:1604.04105v1 [physics.flu-dyn] 14 Apr 2016

Finite element method for extended KdV equations

Anna Karczewska* and Maciej Szczeciński†
Faculty of Mathematics, Computer Science and Econometrics
University of Zielona Góra, Szafrana 4a, 65-246 Zielona Góra, Poland

Piotr Rozmej‡ and Bartosz Boguniewicz§
Institute of Physics, Faculty of Physics and Astronomy
University of Zielona Góra, Szafrana 4a, 65-246 Zielona Góra, Poland
(Dated: April 15, 2016)

The finite element method (FEM) is applied to obtain numerical solutions to a recently derived nonlinear equation for the shallow water wave problem. A weak formulation and the Petrov-Galerkin method are used. It is shown that the FEM gives a reasonable description of the wave dynamics of soliton waves governed by extended KdV equations. Some new results for several cases of bottom shapes are presented. The numerical scheme presented here is suitable for taking into account stochastic effects, which will be discussed in a subsequent paper.

PACS numbers: 02.30.Jr, 05.45.-a, 47.35.Bb, 47.35.Fg
Keywords: Shallow water wave problem, nonlinear equations, second order KdV equations, finite element method, Petrov-Galerkin method.

I. INTRODUCTION

The Korteveg–de Vries equation appears as a model for the propagation of weakly nonlinear dispersive waves in several fields. Among them there are gravity driven waves on a surface of an incompressible irrotational inviscid fluid [7, 8, 15, 22, 30, 35], ion acoustic waves in plasma [15], impulse propagation in electric circuits [30] and so on. In the shallow water wave problem the KdV equation corresponds to the case when the bottom is even. There have been many attempts to study nonlinear waves in the case of an uneven bottom because of its significance, for instance in such phenomena as tsunamis. Among the first papers dealing with a slowly varying bottom are papers of Mei and Le Méhauté [24] and Grimshaw [12]. When taking an appropriate average of vertical variables one arrives at Green-Nagdi type equations [11, 21, 26]. Van Groesen and Pudyaprasetya [29, 34] studied unidirectional waves over a slowly varying bottom within the Hamilton approach, obtaining a forced KdV-type equation. An extensive study of wave propagation over an uneven bottom conducted before 2000 is summarized in Dingemans's monograph [7]. The papers [14, 27, 28] are examples of approaches that combine linear and nonlinear theories. The Gardner equation and the forced KdV equation, were also extensively investigated in this context, see, e.g., [13, 16, 32].

In previous papers, [17, 18] we derived a new KdV-type equation containing terms which come directly from an uneven bottom. These terms, however, appear naturally only if Euler equations for the fluid motion are considered up to second order in small parameters, whereas the KdV equation is obtained in first order approximation. There are no analytic solutions for the above equation. In [17, 18] we presented several cases of numerical simulations for that equation obtained using the finite difference method (FDM) with periodic boundary conditions.

It was demonstrated in [6] that finite element method (FEM) describes properly the dynamics of the KdV equation (6), which is the equation in a moving frame of reference.

The first aim of this paper is to construct an effective FEM method for solving higher order KdV equations, both with even bottom and uneven bottom. The second goal is to compare the results obtained in this numerical scheme with some of the results obtained earlier using the finite difference method in [17] and in [18].

The paper is organized as follows: In section II we review the KdV equation (4), the extended KdV equation (3) and KdV-type equation containing direct terms from bottom variation (1), all expressed in scaled dimensionless variables. In section III the construction of the numerical method for solving these equations within the FEM is described. Coupled sets of nonlinear equations for coefficients of expansion of solutions to these equations in a basis of piecewise linear functions are obtained. In section IV several examples of numerical simulations are presented.

II. PRELIMINARIES

Extended KdV type equations, derived by some of the authors in [17, 18], second order in small parameters, have the following form (written in scaled dimensionless coordinates, in a fixed coordinate system). For the case

* A.Karczewska@wmie.uz.zgora.pl
† m.szczecinski@wmie.uz.zgora.pl
‡ P.Rozmej@if.uz.zgora.pl
§ b.boguniewicz@gmail.com

with an uneven bottom

$$\eta_t + \eta_x + \alpha\frac{3}{2}\eta\eta_x + \beta\frac{1}{6}\eta_{3x} - \frac{3}{8}\alpha^2\eta^2\eta_x + \alpha\beta\left(\frac{23}{24}\eta_x\eta_{2x} + \frac{5}{12}\eta\eta_{3x}\right) + \frac{19}{360}\beta^2\eta_{5x} + \beta\delta\left(-\frac{1}{2\beta}(h\eta)_x + \frac{1}{4}\left(h_{2x}\eta\right)_x - \frac{1}{4}\left(h\eta_{2x}\right)_x\right) = 0. \tag{1}$$

Details of the derivation of the second order equation (1) from the set of Euler equations with appropriate boundary conditions can be found in [17, 18]. In (1), $\eta(x,t)$ stands for a wave profile and $h = h(x)$ denotes a bottom profile. Subscripts are used for notation of partial derivatives, that is, for instance $\eta_{2x} \equiv \frac{\partial^2\eta}{\partial x^2}$, and so on. Small parameters α, β, δ are defined by ratios of the amplitude of the wave profile a, the depth of undisturbed water h_0, average wavelength l and the amplitude of the bottom changes a_h

$$\alpha = \frac{a}{h_0}, \qquad \beta = \left(\frac{h}{l}\right)^2, \qquad \delta = \frac{a_h}{h_0}. \tag{2}$$

For details of the transformation of the original dimensional variables to the nondimensional, scaled ones used here, see, e.g., [4, 17, 18].

It should be emphasized that in equation (1) all three terms originating from an uneven bottom are second order in small parameters. These terms appear from the boundary condition at the bottom which is already in second order with coefficient $\beta\delta$, see equation (5) in [18] or equation (10) in [17]. Then in the final second order equation (1) we write them in the form $\beta\delta(\cdot)$ in order to epmhasize that they all come from the second order perturbation approach. For details we refer to the mentioned papers.

In the case of an even bottom ($\delta = 0$) equation (1) is reduced to the second order KdV type equation

$$\eta_t + \eta_x + \alpha\frac{3}{2}\eta\eta_x + \beta\frac{1}{6}\eta_{3x} - \frac{3}{8}\alpha^2\eta^2\eta_x + \alpha\beta\left(\frac{23}{24}\eta_x\eta_{2x} + \frac{5}{12}\eta\eta_{3x}\right) + \frac{19}{360}\beta^2\eta_{5x} = 0 \tag{3}$$

and when $\beta = \alpha$ it becomes identical to Eq. (21) in [4]. Equation (3) was obtained earlier by Marchant and Smyth [22] and called the *extended KdV* equation.

Limitation to first order approximation in small parameters gives the KdV in a fixed system of coordinates

$$\eta_t + \eta_x + \alpha\frac{3}{2}\eta\eta_x + \beta\frac{1}{6}\eta_{3x} = 0. \tag{4}$$

The standard, mathematical form of the KdV equation is obtained from (4) by transformation to a moving reference frame. Substituting

$$\bar{x} = \sqrt{\frac{3}{2}}(x - t), \qquad \bar{t} = \frac{1}{4}\sqrt{\frac{3}{2}}\,\alpha\, t, \qquad u = \eta, \tag{5}$$

one obtains from (3) the equation

$$u_{\bar{t}} + 6\,u\,u_{\bar{x}} + \frac{\beta}{\alpha}u_{3\bar{x}} = 0, \tag{6}$$

or finally, when $\beta = \alpha$,

$$u_{\bar{t}} + 6\,u\,u_{\bar{x}} + u_{3\bar{x}} = 0. \tag{7}$$

In this paper we attempt to solve numerically the equation (1) for several cases of bottom topography and different initial conditions. In several points we follow the method applied by Debussche and Printems [6]. However, the method is extended to higher order KdV type equations with plain bottom (3) and with bottom fluctuations (1). For both cases we work in a fixed reference system, necessary for a bottom profile depending on the position.

III. NUMERICAL METHOD

The emergence of soliton solutions to the KdV equation was observed in numerics fifty years ago by [38]. Several numerical methods used for solving the KdV equation are discussed in [33]. Among them are the finite difference explicit method [38], the finite difference implicit method [10] and several versions of the pseudospectral method, as in [9]. It is also worth mentioning papers using the FEM and Galerkin methods [3, 5]. Most numerical applications use periodic boundary conditions, but there exist also works that apply Dirichlet boundary conditions on a finite interval [31, 36, 37].

The authors are trying to construct a method which will be applicable not only for the numerical simulation of an evolution of nonlinear waves governed by equations (1) or (3) but also for their stochastic versions. Such stochastic equations will be studied in the next paper. Since stochastic noise is irregular, solutions are not necessarily smooth, neither in time nor space. A finite element method (FEM) seems to be suitable for such a case.

A. Time discretization

We have adapted the Crank–Nicholson scheme for time evolution, beginning with the KdV equation (4) in a fixed coordinate system. Note that $\eta\eta_x = \frac{1}{2}(\eta^2)_x$. Denote also $v := \eta_x$ and $w := v_x$. Let us choose time step τ. Then the KdV equation (4) in the Crank–Nicholson scheme can be written as a set of coupled first order differential

equations

$$\eta^{n+1}-\eta^n+\tau\left(\frac{\partial}{\partial x}\eta^{n+\frac{1}{2}}+\frac{3\alpha}{4}\frac{\partial}{\partial x}(\eta^{n+\frac{1}{2}})^2+\frac{\beta}{6}w^{n+\frac{1}{2}}\right)=0, \tag{8}$$
$$\frac{\partial}{\partial x}\eta^{n+\frac{1}{2}}=v^{n+\frac{1}{2}},$$
$$\frac{\partial}{\partial x}v^{n+\frac{1}{2}}=w^{n+\frac{1}{2}},$$

where

$$\begin{aligned}\eta^{n+\frac{1}{2}} &= \tfrac{1}{2}\left(\eta^{n+1}+\eta^n\right),\\ v^{n+\frac{1}{2}} &= \tfrac{1}{2}\left(v^{n+1}+v^n\right),\\ w^{n+\frac{1}{2}} &= \tfrac{1}{2}\left(w^{n+1}+w^n\right).\end{aligned} \tag{9}$$

For second order equations (1) or (3) we need to introduce two new auxiliary variables: $p := w_x$ and $q := p_x$. Note that $\eta^2\eta_x = \frac{1}{3}(\eta^3)_x$, $\eta_x\eta_{2x} = \frac{1}{2}(\eta_x^2)_x = \frac{1}{2}(v^2)_x$. Moreover, $\eta_{5x} = q = p_x$ and

$$\frac{23}{24}\eta_x\eta_{2x}+\frac{5}{12}\eta\eta_{3x}=\frac{13}{48}(v^2)_x+\frac{5}{12}(\eta w)_x.$$

This setting allows us to write the Crank–Nicholson scheme for (3) as the following set of first order equations

$$\begin{aligned}&\eta^{n+1}-\eta^n+\\ &+\tau\frac{\partial}{\partial x}\left[\eta^{n+\frac{1}{2}}+\frac{3\alpha}{4}\left(\eta^{n+\frac{1}{2}}\right)^2+\frac{\beta}{6}w^{n+\frac{1}{2}}\right.\\ &-\frac{1}{8}\alpha^2\left(\eta^{n+\frac{1}{2}}\right)^3+\alpha\beta\left(\frac{13}{48}\left(v^{n+\frac{1}{2}}\right)^2\right.\\ &\left.\left.+\frac{5}{12}\left(\eta^{n+\frac{1}{2}}w^{n+\frac{1}{2}}\right)\right)+\frac{19}{360}\beta^2\left(q^{n+\frac{1}{2}}\right)\right]=0,\end{aligned} \tag{10}$$
$$\frac{\partial}{\partial x}\eta^{n+\frac{1}{2}}-v^{n+\frac{1}{2}}=0,$$
$$\frac{\partial}{\partial x}v^{n+\frac{1}{2}}-w^{n+\frac{1}{2}}=0,$$
$$\frac{\partial}{\partial x}w^{n+\frac{1}{2}}-p^{n+\frac{1}{2}}=0,$$
$$\frac{\partial}{\partial x}p^{n+\frac{1}{2}}-q^{n+\frac{1}{2}}=0,$$

where

$$\begin{aligned}p^{n+\frac{1}{2}} &= \tfrac{1}{2}\left(p^{n+1}+p^n\right),\\ q^{n+\frac{1}{2}} &= \tfrac{1}{2}\left(q^{n+1}+q^n\right).\end{aligned} \tag{11}$$

For the second order KdV type equation with an uneven bottom (1) the first equation in the set (10) has to be supplemented by terms originating from bottom variations, yielding

$$\begin{aligned}&\eta^{n+1}-\eta^n+\\ &+\tau\frac{\partial}{\partial x}\left[\eta^{n+\frac{1}{2}}+\frac{3\alpha}{4}\left(\eta^{n+\frac{1}{2}}\right)^2+\frac{\beta}{6}w^{n+\frac{1}{2}}\right.\\ &-\frac{1}{8}\alpha^2\left(\eta^{n+\frac{1}{2}}\right)^3+\alpha\beta\left(\frac{13}{48}\left(v^{n+\frac{1}{2}}\right)^2\right.\\ &\left.\left.+\frac{5}{12}\left(\eta^{n+\frac{1}{2}}w^{n+\frac{1}{2}}\right)\right)+\frac{19}{360}\beta^2\left(q^{n+\frac{1}{2}}\right)\right.\\ &\left.\frac{1}{4}\beta\delta\left(-\frac{2}{\beta}\left(h^{n+\frac{1}{2}}\eta^{n+\frac{1}{2}}\right)\right.\right.\\ &\left.\left.+\eta^{n+\frac{1}{2}}g^{n+\frac{1}{2}}+h^{n+\frac{1}{2}}w^{n+\frac{1}{2}}\right)\right]=0,\end{aligned} \tag{12}$$

where $g := h_{xx}$.

Below we focus on the second order equations (3) and (10), pointing out contributions from bottom variation later.

B. Space discretization

Following the arguments given by Debussche and Printems [6] we apply the Petrov-Galerkin discretization and finite element method. We use piecewise linear shape functions and piecewise constant test functions. We consider wave motion on the interval $x \in [0, L]$ with periodic boundary conditions. Given $N \in \mathbb{N}$, then we use a mesh M_χ of points $x_j = j\chi$, $j = 0, 1, \ldots, N$, where $\chi = L/N$. Let V_χ^1 which is a space of piecewise linear functions $\varphi_j(x)$, such that $\varphi_j(0) = \varphi_j(L)$, defined as

$$\varphi_j(x)=\begin{cases}\frac{1}{\chi}(x-x_{j-1}) & \text{if } x\in[x_{j-1},x_j]\\ \frac{1}{\chi}(x_{j+1}-x) & \text{if } x\in[x_j,x_{j+1}]\\ 0 & \text{otherwise.}\end{cases} \tag{13}$$

As test functions we have chosen the space of piecewise constant functions $\psi_j(x) \in V_\chi^0$, where

$$\psi_j(x)=\begin{cases}1 & \text{if } x\in[x_j,x_{j+1})\\ 0 & \text{otherwise.}\end{cases} \tag{14}$$

An approximate solution and its derivatives may be written as an expansion in the basis (13)

$$\begin{aligned}\eta_\chi^n(x) &= \textstyle\sum_{j=1}^N a_j^n\,\varphi_j(x),\\ v_\chi^n(x) &= \textstyle\sum_{j=1}^N b_j^n\,\varphi_j(x),\\ w_\chi^n(x) &= \textstyle\sum_{j=1}^N c_j^n\,\varphi_j(x),\\ p_\chi^n(x) &= \textstyle\sum_{j=1}^N d_j^n\,\varphi_j(x),\\ q_\chi^n(x) &= \textstyle\sum_{j=1}^N e_j^n\,\varphi_j(x),\end{aligned} \tag{15}$$

where $a_j^n, b_j^n, c_j^n, d_j^n, e_j^n$ are expansion coefficients. There-

fore, in a weak formulation we can write (8) as

$$\begin{aligned}
&\left(\eta_\chi^{n+1}-\eta_\chi^n,\psi_i\right)+\tau\left\{\left(\partial_x\eta_\chi^{n+\frac12},\psi_i\right)\right.\\
&+\frac{3\alpha}{4}\left(\partial_x\left(\eta_\chi^{n+\frac12}\right)^2,\psi_i\right)+\frac{\beta}{6}\left(\partial_x w_\chi^{n+\frac12},\psi_i\right)\\
&-\frac18\alpha^2\left(\partial_x\left(\eta_\chi^{n+\frac12}\right)^3,\psi_i\right)\\
&+\alpha\beta\left[\frac{13}{48}\left(\partial_x\left(v_\chi^{n+\frac12}\right)^2,\psi_i\right)\right.\\
&\left.+\frac{5}{12}\left(\partial_x\left(\eta_\chi^{n+\frac12}w_\chi^{n+\frac12}\right),\psi_i\right)\right]\\
&\left.+\frac{19}{360}\beta^2\left(\partial_x\left(q_\chi^{n+\frac12}\right),\psi_i\right)\right\}=0,\\
&\left(\partial_x\eta_\chi^{n+\frac12},\psi_i\right)-\left(v_\chi^{n+\frac12},\psi_i\right)=0,\\
&\left(\partial_x v_\chi^{n+\frac12},\psi_i\right)-\left(w_\chi^{n+\frac12},\psi_i\right)=0,\\
&\left(\partial_x w_\chi^{n+\frac12},\psi_i\right)-\left(p_\chi^{n+\frac12},\psi_i\right)=0,\\
&\left(\partial_x p_\chi^{n+\frac12},\psi_i\right)-\left(q_\chi^{n+\frac12},\psi_i\right)=0,
\end{aligned}\tag{16}$$

for any $i=1,\dots,N$, where for abbreviation ∂_x is used for $\frac{\partial}{\partial x}$. In (16) and below scalar products are defined by appropriate integrals

$$(f,g):=\int_0^L f(x)g(x)dx.$$

In the case of equation (1), the first equation of the set (16) has to be supplemented inside the bracket { } by the terms

$$\begin{aligned}
&+\frac14\beta\delta\left(\partial_x\left[-\frac{2}{\beta}\left(h^{n+\frac12}\eta_\chi^{n+\frac12}\right)\right.\right.\\
&\left.\left.+\eta_\chi^{n+\frac12}g^{n+\frac12}+h^{n+\frac12}w_\chi^{n+\frac12}\right],\psi_i\right).
\end{aligned}\tag{17}$$

Insertion of (15) into (16) yields a system of coupled linear equations for coefficients $a_j^n,b_j^n,c_j^n,d_j^n,e_j^n$. The solution to this system supplies an approximate solution to (3) given in the mesh points x_j.

1. KdV equation

In order to demonstrate the construction of the matrices involved we limit at this point our considerations to the first order equation (4). It means that we drop temporarily in (16) terms of second order, that is, the terms with $\alpha^2,\alpha\beta,\beta^2$. Equations with p and q do not apply because η_{4x} and η_{5x} do not appear in (4). This leads to equations

$$\begin{aligned}
&\sum_{j=1}^N(a_j^{n+1}-a_j^n)(\varphi_j,\psi_i)+\tau\frac12\sum_{j=1}^N(b_j^{n+1}+b_j^n)(\varphi_j,\psi_i)\\
&+\tau\alpha\frac{3}{16}\sum_{j=1}^N\sum_{k=1}^N(a_j^{n+1}+a_j^n)(a_k^{n+1}+a_k^n)\\
&\times(\varphi_j'\varphi_k+\varphi_j\varphi_k',\psi_i)\\
&+\tau\beta\frac{1}{12}\sum_{j=1}^N(c_j^{n+1}+c_j^n)(\varphi_j,\psi_i)=0,\\
&\sum_{j=1}^N\left[(a_j^{n+1}+a_j^n)(\varphi_j',\psi_i)-(b_j^{n+1}+b_j^n)(\varphi_j,\psi_i)\right]=0,\\
&\sum_{j=1}^N\left[(b_j^{n+1}+b_j^n)(\varphi_j',\psi_i)-(c_j^{n+1}+c_j^n)(\varphi_j,\psi_i)\right]=0.
\end{aligned}\tag{18}$$

Define

$$\begin{aligned}
&C_{ij}^{(1)}:=(\varphi_j,\psi_i),\qquad &&C_{ij}^{(2)}:=(\varphi_j',\psi_i),\\
&C_{ijk}^{(3)}:=(\varphi_j'\varphi_k+\varphi_j\varphi_k',\psi_i),
\end{aligned}\tag{19}$$

where $\varphi_j'=\frac{d\varphi}{dx}(x_j)$. Simple integration shows that

$$C_{ij}^{(1)}=\begin{cases}\frac12\chi & \text{if}\quad i=j\vee i=j-1\\ 0 & \text{otherwise,}\end{cases}\tag{20}$$

$$C_{ij}^{(2)}=\begin{cases}-1 & \text{if}\quad i=j\\ 1 & \text{if}\quad i=j-1\\ 0 & \text{otherwise.}\end{cases}\tag{21}$$

Similarly one obtains

$$C_{ijk}^{(3)}=C_{ij}^{(2)}\,\delta_{jk}.\tag{22}$$

The property (22) reduces the double sum in the term with $\tau\alpha\frac{3}{16}$ to the single one of the square of $(a_j^{n+1}+a_j^n)$. Insertion of (20)–(22) into (18) gives

$$\begin{aligned}
&\sum_{j=1}^N\left[(a_j^{n+1}-a_j^n)C_{ij}^{(1)}+\tau\left(\frac12(b_j^{n+1}+b_j^n)C_{ij}^{(1)}\right.\right.\\
&\left.\left.+\alpha\frac{3}{16}(a_j^{n+1}+a_j^n)^2C_{ij}^{(2)}+\beta\frac{1}{12}(c_j^{n+1}+c_j^n)C_{ij}^{(2)}\right)\right]=0,\\
&\sum_{j=1}^N\left[(a_j^{n+1}+a_j^n)C_{ij}^{(2)}-(b_j^{n+1}+b_j^n)C_{ij}^{(1)}\right]=0,\\
&\sum_{j=1}^N\left[(b_j^{n+1}+b_j^n)C_{ij}^{(2)}-(c_j^{n+1}+c_j^n)C_{ij}^{(1)}\right]=0.
\end{aligned}\tag{23}$$

Define the $3N$-dimensional vector of expansion coefficients

$$X^n=\begin{pmatrix}A^n\\B^n\\C^n\end{pmatrix},\tag{24}$$

where

$$A^n = \begin{pmatrix} a_1^n \\ a_2^n \\ \vdots \\ a_N^n \end{pmatrix},\ B^n = \begin{pmatrix} b_1^n \\ b_2^n \\ \vdots \\ b_N^n \end{pmatrix},\ C^n = \begin{pmatrix} c_1^n \\ c_2^n \\ \vdots \\ c_N^n \end{pmatrix}. \quad (25)$$

In (23), $A^{n+1}, B^{n+1}, C^{n+1}$ represent the unknown coefficients and A^n, B^n, C^n the known ones. Note that the system (23) is nonlinear. The single nonlinear term is quadratic in unknown coefficients. For the second order equations (3) and (1) there are more nonlinear terms.

In an abbreviated form the set (23) can be written as

$$F_i(X^{n+1}, X^n) = 0, \quad i = 1, 2, \ldots, 3N. \quad (26)$$

Since this equation is nonlinear we can use the Newton method for each time step. That is, we find X^{n+1} by iterating the equation

$$(X^{n+1})_{m+1} = (X^{n+1})_m + J^{-1}(X^{n+1})_m = 0, \quad (27)$$

where J^{-1} is the inverse of the Jacobian of $F(X^{n+1}, X^n)$ (26). Choosing $(X^{n+1})_0 = X^n$ we obtain the approximate solution to (26), $(X^{n+1})_m$ in $m = 3 - 5$ iterations with very good precision. The Jacobian itself is a particular $(3N \times 3N)$ sparse matrix with the following block structure

$$J = \begin{pmatrix} (A_a) & (A_b) & (A_c) \\ (C2) & -(C1) & (0) \\ (0) & (C2) & -(C1) \end{pmatrix}, \quad (28)$$

where each block $(\cdot)$ is a two-diagonal sparse $(N \times N)$ matrix. The matrix A_a is given by

$$A_a = \begin{pmatrix} a_1^1 & 0 & 0 & \cdots & 0 & a_{N-1}^1 & a_N^1 \\ a_1^2 & a_2^2 & 0 & \cdots & 0 & 0 & a_N^2 \\ 0 & a_2^3 & a_3^3 & 0 & \cdots & 0 & 0 \\ \vdots & \vdots & \vdots & \ddots & \vdots & \vdots & \vdots \\ 0 & 0 & \cdots & a_{N-4}^{N-3} & a_{N-3}^{N-3} & 0 & 0 \\ 0 & 0 & \cdots & 0 & a_{N-3}^{n-2} & a_{N-2}^{N-2} & 0 \\ a_1^N & 0 & \cdots & 0 & 0 & a_N^{N-1} & a_N^n \end{pmatrix}. \quad (29)$$

In (29) the nonzero elements of A_a are given by

$$a_j^i = \frac{\partial F_i}{\partial a_j^{n+1}}, \quad (30)$$

where F is given by (26). The elements in the upper right and lower left corners result from periodic boundary conditions. Matrices A_b and A_c have the same structure as A_a, with only elements a_j^i having to be replaced by $b_j^i = \frac{\partial F_i}{\partial b_j^{n+1}}$ and $c_j^i = \frac{\partial F_i}{\partial c_j^{n+1}}$, respectively.

Matrices $C1$ and $C2$ are constant. They are defined as

$$Ck = \begin{pmatrix} C_{11}^{(k)} & 0 & \cdots & C_{11}^{(k)} & C_{1N}^{(k)} \\ C_{21}^{(k)} & C_{22}^{(k)} & \cdots & 0 & C_{2N}^{(k)} \\ \vdots & \vdots & \ddots & \vdots & \vdots \\ 0 & 0 & \cdots & C_{N-1N-1}^{(k)} & 0 \\ C_{N1}^{(k)} & 0 & \cdots & C_{N-1N}^{(k)} & C_{NN}^{(k)} \end{pmatrix}, \quad (31)$$

where $k = 1, 2$.

2. *Extended KdV equation (3)*

For the second order equation (3) there are more nonlinear terms. These are terms with α^2 and $\alpha\beta$. According to the Petrov–Galerkin scheme we get for the term with α^2

$$\begin{aligned} \partial_x \left(\eta^{n+\frac{1}{2}}\right)^3 &= \frac{1}{8}\left(\partial_x \sum_{j=1}^{N} \left(a_j^{n+1} + a_j^n\right)\varphi_j\right)^3 \\ &= \frac{1}{8}\partial_x \sum_{j=1}^{N}\sum_{k=1}^{N}\sum_{l=1}^{N}[a_j^{n+1} + a_j^n][a_k^{n+1} + a_k^n][a_l^{n+1} + a_l^n] \\ &\qquad \times\varphi_j\varphi_k\varphi_l \quad (32) \\ &= \frac{1}{8}\sum_{j=1}^{N}\sum_{k=1}^{N}\sum_{l=1}^{N}[a_j^{n+1} + a_j^n][a_k^{n+1} + a_k^n][a_l^{n+1} + a_l^n] \\ &\qquad \times\left(\varphi_j'\varphi_k\varphi_l + \varphi_j\varphi_k'\varphi_l + \varphi_j\varphi_k\varphi_l'\right). \end{aligned}$$

Denote

$$C_{ijkl}^{(4)} := \left(\left[\varphi_j'\varphi_k\varphi_l + \varphi_j\varphi_k'\varphi_l + \varphi_j\varphi_k\varphi_l'\right], \psi_i\right). \quad (33)$$

As with $C_{ijk}^{(3)}$ in (22) the following property holds

$$C_{ijkl}^{(4)} = C_{ij}^2\, \delta_{jk}\, \delta_{kl}. \quad (34)$$

In a similar way, for terms with $\alpha\beta$ we obtain

$$\begin{aligned} &\partial_x \left(v^{n+\frac{1}{2}}\right)^2 \quad (35) \\ &= \frac{1}{4}\partial_x \left(\sum_{j=1}^{N}\left(b_j^{n+1} + b_j^n\right)\varphi_j \sum_{k=1}^{N}\left(b_k^{n+1} + b_k^n\right)\varphi_k\right) \\ &= \frac{1}{4}\sum_{j=1}^{N}\sum_{k=1}^{N}[b_j^{n+1} + a_j^n][b_k^{n+1} + b_k^n]\left(\varphi_j'\varphi_k + \varphi_j\varphi_k'\right) \end{aligned}$$

and

$$\begin{aligned} &\partial_x \left(\eta^{n+\frac{1}{2}} w^{n+\frac{1}{2}}\right) \quad (36) \\ &= \frac{1}{4}\partial_x \left(\sum_{j=1}^{N}\left(a_j^{n+1} + a_j^n\right)\varphi_j \sum_{k=1}^{N}\left(a_k^{n+1} + a_k^n\right)\varphi_k\right) \\ &= \frac{1}{4}\sum_{j=1}^{N}\sum_{k=1}^{N}[a_j^{n+1} + a_j^n][b_k^{n+1} + b_k^n]\left(\varphi_j'\varphi_k + \varphi_j\varphi_k'\right). \end{aligned}$$

The scalar products appearing in the terms proportional to α^2 and $\alpha\beta$ are already defined: $\left(\left(\varphi_j'\varphi_k + \varphi_j\varphi_k'\right), \psi_i\right) = C_{ijk}^{(3)}$.

Due to properties (34) and (22) triple and double sums reduce to single ones. With these settings the second

order KdV equation (16) gives the following system of equations

$$\sum_{j=1}^{N}\Big\{(a_j^{n+1}-a_j^n)C_{ij}^{(1)}+\tau\Big[\frac{1}{2}(b_j^{n+1}+b_j^n)C_{ij}^{(1)} \tag{37}$$
$$+\Big(\alpha\frac{3}{16}(a_j^{n+1}+a_j^n)^2+\beta\frac{1}{12}(c_j^{n+1}+c_j^n)$$
$$-\alpha^2\frac{1}{64}(a_j^{n+1}+a_j^n)^3+\alpha\beta\frac{13}{192}(b_j^{n+1}+b_j^n)^2$$
$$+\alpha\beta\frac{5}{96}(a_j^{n+1}+a_j^n)(c_j^{n+1}+c_j^n)$$
$$+\beta^2\frac{19}{720}(e_j^{n+1}+e_j^n)\Big)C_{ij}^{(2)}\Big]\Big\}=0,$$
$$\sum_{j=1}^{N}\Big[(a_j^{n+1}+a_j^n)C_{ij}^{(2)}-(b_j^{n+1}+b_j^n)C_{ij}^{(1)}\Big]=0,$$
$$\sum_{j=1}^{N}\Big[(b_j^{n+1}+b_j^n)C_{ij}^{(2)}-(c_j^{n+1}+c_j^n)C_{ij}^{(1)}\Big]=0,$$
$$\sum_{j=1}^{N}\Big[(c_j^{n+1}+c_j^n)C_{ij}^{(2)}-(d_j^{n+1}+d_j^n)C_{ij}^{(1)}\Big]=0,$$
$$\sum_{j=1}^{N}\Big[(b_j^{n+1}+b_j^n)C_{ij}^{(2)}-(e_j^{n+1}+e_j^n)C_{ij}^{(1)}\Big]=0,$$

where $i=1,2,\ldots,N$.

In this case the vector of expansion coefficients X^n is $5N$-dimensional

$$X^n=\begin{pmatrix}A^n\\B^n\\C^n\\D^n\\E^n\end{pmatrix}, \tag{38}$$

where A^n, B^n and C^n are already defined in (25) and

$$D^n=\begin{pmatrix}d_1^n\\d_2^n\\\vdots\\d_N^n\end{pmatrix},\ E^n=\begin{pmatrix}e_1^n\\e_2^n\\\vdots\\e_N^n\end{pmatrix}. \tag{39}$$

The Jacobian becomes now $(5N\times 5N)$ dimensional. Its structure, however, is similar to (28), that is

$$J=\begin{pmatrix}(A_a)&(A_b)&(A_c)&(0)&(A_e)\\(C2)&-(C1)&(0)&(0)&(0)\\(0)&(C2)&-(C1)&(0)&(0)\\(0)&(0)&(C2)&-(C1)&(0)\\(0)&(0)&(0)&(C2)&-(C1)\end{pmatrix}, \tag{40}$$

where the matrices $(A_a),(A_b),(A_c)$ are defined as previously and $(A_e)_{ij}=\frac{\partial F_i}{\partial e_j^{n+1}}$. Now F_i represents the set (37) which contains four nonlinear terms.

3. Extended KdV equation with uneven bottom

For the extended KdV with non-flat bottom we have to include into (37) three additional terms contained in the last line of formula (1). Expanding the bottom function $h(x)$ and its second derivative $h_{2x}(x)$ in the basis $\{\varphi_j(x)\}$

$$h(x)=\sum_{j=1}^{N}H0_j\varphi_j(x),\quad h_{2x}(x)=\sum_{j=1}^{N}H2_j\varphi_j(x) \tag{41}$$

we can write the terms mentioned above in the following form

$$\partial_x\Big(h\eta^{n+\frac{1}{2}}\Big) \tag{42}$$
$$=\frac{1}{2}\sum_{j=1}^{N}\sum_{k=1}^{N}H0_j\ \left(a_k^{n+1}+a_k^n\right)\left(\varphi_j'\varphi_k+\varphi_j\varphi_k'\right),$$
$$\partial_x\Big(h_{2x}\eta^{n+\frac{1}{2}}\Big) \tag{43}$$
$$=\frac{1}{2}\sum_{j=1}^{N}\sum_{k=1}^{N}H2_j\ \left(a_k^{n+1}+a_k^n\right)\left(\varphi_j'\varphi_k+\varphi_j\varphi_k'\right).$$
$$\partial_x\Big(h\eta_{2x}^{n+\frac{1}{2}}\Big) \tag{44}$$
$$=\frac{1}{2}\sum_{j=1}^{N}\sum_{k=1}^{N}H0_j\ \left(c_k^{n+1}+c_k^n\right)\left(\varphi_j'\varphi_k+\varphi_j\varphi_k'\right).$$

Since

$$\left(\left(\varphi_j'\varphi_k+\varphi_j\varphi_k'\right),\psi_i\right)=C^{(3)}(i,j,k)=C^{(2)}(i,j)\,\delta_{jk},$$

terms proportional to $\beta\delta$ can be reduced to single sums like those proportional to $\alpha^2,\alpha\beta$ and β^2 discussed in previous subsections. Finally one obtains (1) as a system of

coupled nonlinear equations ($i = 1, 2, \ldots, N$)

$$\sum_{j=1}^{N}\Bigg\{(a_j^{n+1}-a_j^n)C_{ij}^{(1)}+\tau\Bigg[\frac{1}{2}(b_j^{n+1}+b_j^n)C_{ij}^{(1)} \tag{45}$$
$$+\Bigg(\alpha\frac{3}{16}(a_j^{n+1}+a_j^n)^2+\beta\frac{1}{12}(c_j^{n+1}+c_j^n)$$
$$-\alpha^2\frac{1}{64}(a_j^{n+1}+a_j^n)^3+\alpha\beta\Bigg(\frac{13}{192}(b_j^{n+1}+b_j^n)^2$$
$$+\frac{5}{96}(a_j^{n+1}+a_j^n)(c_j^{n+1}+c_j^n)\Bigg)+\beta^2\frac{19}{720}(e_j^{n+1}+e_j^n)$$
$$-\frac{1}{4}\delta H0_j\,\left(a_k^{n+1}+a_k^n\right)+\frac{1}{8}\beta\delta H2_j\,\left(a_k^{n+1}+a_k^n\right)$$
$$-\frac{1}{8}\beta\delta H0_j\,(c_j^{n+1}+c_j^n)\Bigg)C_{ij}^{(2)}\Bigg]\Bigg\}=0,$$
$$\sum_{j=1}^{N}\left[(a_j^{n+1}+a_j^n)C_{ij}^{(2)}-(b_j^{n+1}+b_j^n)C_{ij}^{(1)}\right]=0,$$
$$\sum_{j=1}^{N}\left[(b_j^{n+1}+b_j^n)C_{ij}^{(2)}-(c_j^{n+1}+c_j^n)C_{ij}^{(1)}\right]=0,$$
$$\sum_{j=1}^{N}\left[(c_j^{n+1}+c_j^n)C_{ij}^{(2)}-(d_j^{n+1}+d_j^n)C_{ij}^{(1)}\right]=0,$$
$$\sum_{j=1}^{N}\left[(b_j^{n+1}+b_j^n)C_{ij}^{(2)}-(e_j^{n+1}+e_j^n)C_{ij}^{(1)}\right]=0.$$

In this case the structures of the vector X^n and all matrices remain the same as in (38)–(40). However the matrix elements in matrices A_a and A_c are now different to those in the previous subsection III B 2, due to new terms in (45).

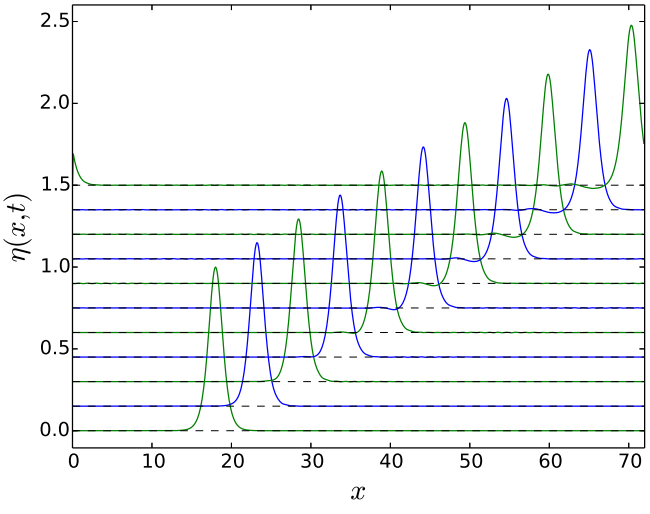

FIG. 1. Time evolution of the initial KdV soliton according to the extended KdV equation (3). Profiles are obtained by numerical solution of the set of equations (37). Dashed lines represent the undisturbed fluid surface.

IV. NUMERICAL SIMULATIONS

It was demonstrated in [6] that the method described in the previous section works reasonably well for the KdV equation (7). Our aim was to apply the finite element method in order to numerically solve the second order equations with a flat bottom (3) and with an uneven bottom (1). There exist two kinds of solutions to KdV equations: soliton (in general, multi-soliton) solutions and periodic solutions called cnoidal waves, see, e.g. [7, 35]. In subsections IV A and IV B we present some examples of numerical simulations for soliton solutions, whereas in the subsection IV C, some examples for cnoidal solutions.

A. Extended KdV equation (3)

In Fig. 1 we present several steps of the time evolution of the soliton wave (at $t = 0$ it is the KdV soliton) according the the extended KdV equation (3) and numerical scheme (37). The mesh size is $N = 720$, with a time step $\tau = \chi^2$, and parameters $\alpha = \beta = 0.1$. Plotted are the calculated profiles of the wave $\eta(x, t_k)$ where $t_k = 5{\cdot}k$, $k = 0, 1, ..., 10$. In order to avoid overlaps of profiles at different time instants each subsequent profile is shifted up by 0.15 with respect to the previous one. This convention is used in Figs. 2 and 3, as well. Here and in the next figures the dashed lines represent the undisturbed fluid surface. As the initial condition we chose the standard KdV soliton centered at $x_0 = 18$. That is, in the applied units, $\eta(x, t = 0) = \mathrm{sech}^2\left[\frac{\sqrt{3}}{2}(x - x_0)\right]$. Note, that since we use scaled variables and definition (2) the amplitude of the soliton is equal 1. In Figs. 2-4 we use the same initial conditions.

The soliton motion shown in Fig. 1 is in agreement with the numerical results obtained with the finite difference method in [17, 18]. With parameters $\alpha = \beta = 0.1$ the resulting distortion of the KdV soliton due to second order terms in (3), (37) is in the form of a small amplitude wavetrain created behind the main wave.

B. Uneven bottom

We may question whether the FEM numerical approach to the extended KdV (45) is precise enough to reveal the details of soliton distortion caused by a varying bottom. The examples plotted in Figs. 2-4 show that it is indeed the case. In all the presented calculations the amplitude of the bottom variations is $\delta = 0.2$. The bottom profile is plotted as a black line below zero on a different scale than the wave profile.

In Fig. 2 the motion of the KdV soliton over a wide bottom hump of Gaussian shape is presented. Here, the bottom function is $h(x) = \delta\exp(-(\frac{x-36}{7})^2)$. In the scaled variables the undisturbed surface of the water (dashed lines) is at $y = 0$. The soliton profiles shown in Fig. 2

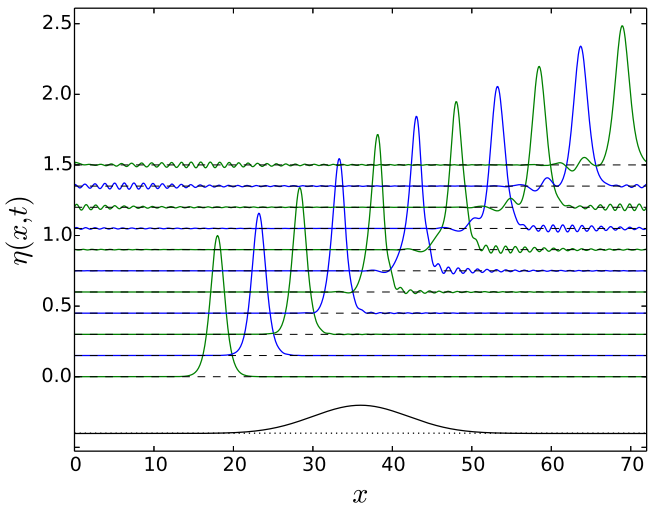

FIG. 2. Time evolution of the initial KdV soliton governed by the extended KdV equation (1) when the bottom has one hump. Here and in the following figures the dotted line shows the position of (the) undisturbed bottom.

are almost the same as the profiles obtained with the finite differences method (FDM) used in [17, 18]. There are small differences due to smaller precision of our FEM calculations. The FEM allows for the use of larger time steps then FDM. However, in the FEM the computing time grows rapidly with the increase in the number N of the mesh, since calculation of the inverse of the Jacobian $(5N \times 5N)$ matrices becomes time consuming.

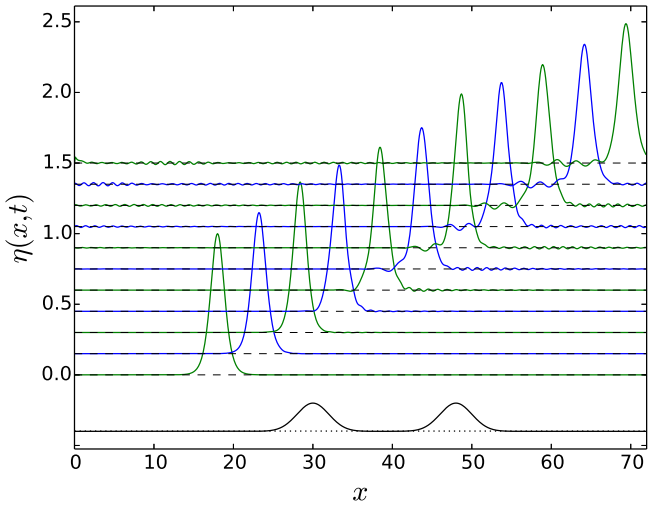

FIG. 3. Time evolution of the initial KdV soliton governed by the extended KdV equation (1) when the bottom has two narrow humps.

Fig. 3 displays the motion of the KdV soliton above a double humped Gaussian shaped bottom defined by $h(x) = \delta[\exp(-(\frac{x-30}{6\sqrt{2}})^2) + \exp(-(\frac{x-48}{6\sqrt{2}})^2)$. Here both Gaussians are rather narrow and therefore distortions of the wave shape from the ideal soliton are smaller than those in Fig. 2.

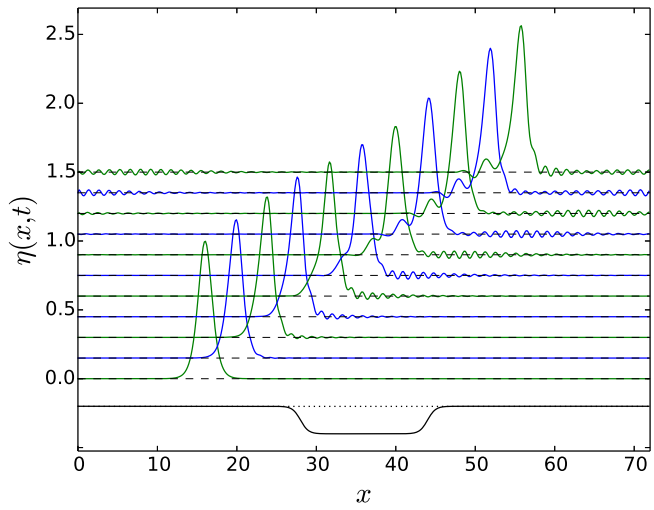

FIG. 4. Time evolution of the initial KdV soliton governed by the extended KdV equation (1) when the bottom has a well.

In Fig. 4 we see the influence of a bottom well with horizontal size extending the soliton's wavelength. The bottom function is chosen as $h(x) = 1 - \frac{\delta}{2}[\tanh(x-28) + \tanh(44-x)]$ symmetric with respect to the center of the x interval. Fig. 4 shows that during the motion above smooth obstacles two effects appear. First, some additional 'waves' of small amplitude, but moving faster than the main solitary wave appear. Second, a wave of smaller amplitude and smaller velocity appears behind the main wave. Both these properties were observed and described in detail in our previous paper [18].

C. Motion of cnoidal waves

The cnoidal solutions to KdV equation are expressed by the Jacobi elliptic cn^2 function. The explicit formula for cnoidal solutions is, see, e.g., [7]:

$$\eta(x,t) = \eta_2 + H\mathrm{cn}^2\left(\left.\frac{x-ct}{\Delta}\right| m\right), \qquad (46)$$

where

$$\eta_2 = \frac{H}{m}\left(1 - m - \frac{E(m)}{K(m)}\right), \quad \Delta = h\sqrt{\frac{4mh}{3H}}, \qquad (47)$$

and

$$c = \sqrt{gh}\left[1 + \frac{H}{mh}\left(1 - \frac{m}{2} - \frac{3E(m)}{2K(m)}\right)\right]. \qquad (48)$$

The solution (46)-(48) is written in dimensional quantities, where H is the wave height, h is mean water depth, g is the gravitational acceleration and m is an elliptic parameter. $K(m)$ and $E(m)$ are complete elliptic integrals

of the first kind and the second kind, respectively. The value of $m \in [0,1]$ governs the shape of the wave.

For $m \to 0$ the cnoidal solution converges to a cosine function. For $m \to 1$ the cnoidal wave forms peaked crests and flat troughs, such that for $m = 1$ the distance between crests increases to infinity and the cnoidal wave converges to a soliton solution.

For (1) and (3) we have to express the formulas (46)-(48) in dimensionless variables.

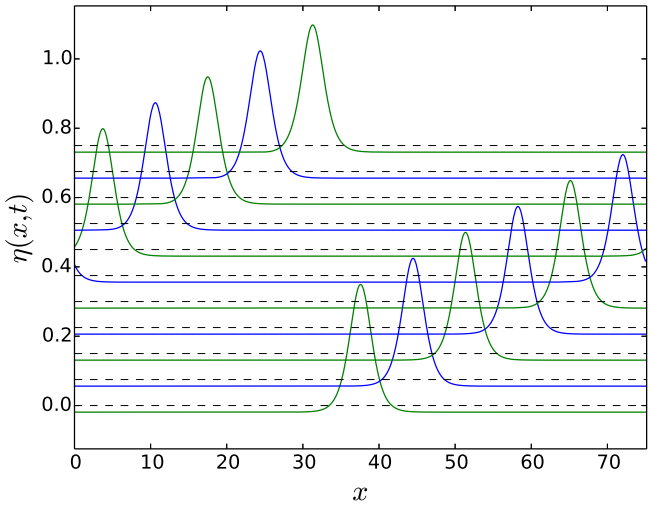

FIG. 5. Time evolution of the initial KdV cnoidal wave governed by the extended KdV equation (3) and numerical scheme (37).

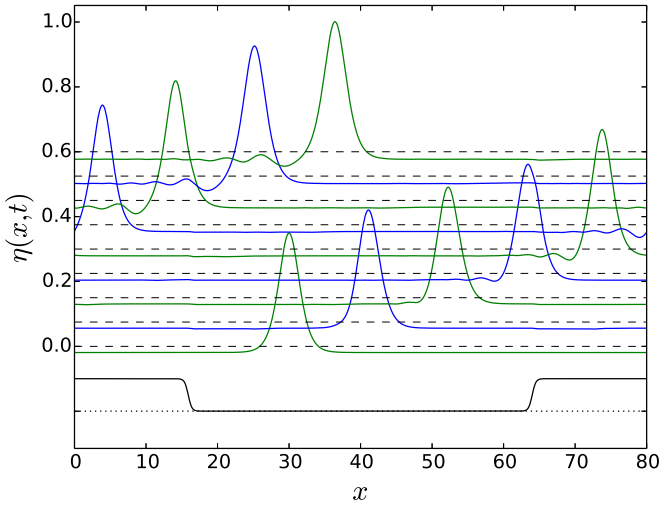

FIG. 6. Time evolution of the initial KdV cnoidal wave governed by the extended KdV equation (1). The bottom function is here $h(x) = \frac{1}{2}[-\tanh(2(x-8.6)-\frac{1}{2}) + \tanh(2(x-66.5552)-\frac{1}{2})]$.

Fig. 5 shows the time evolution of the cnoidal wave according to the extended KdV equation (3), that is, the second order KdV equation with flat bottom. The

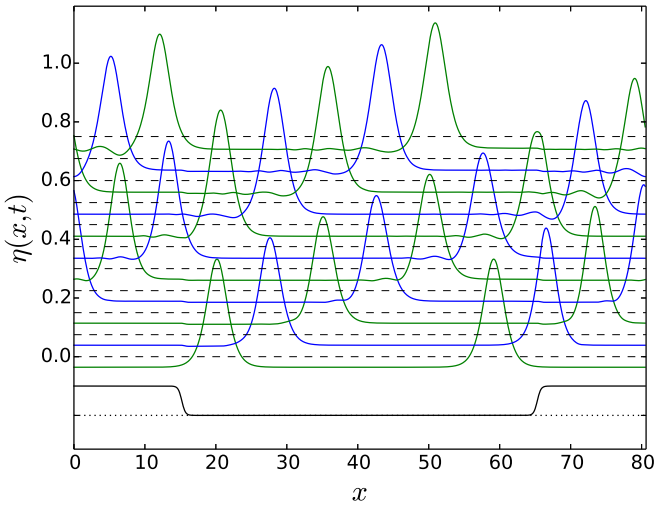

FIG. 7. Time evolution of the initial KdV cnoidal wave governed by the extended KdV equation (1). The bottom function is here $h(x) = \frac{1}{2}[-\tanh(2(x-13.3)-\frac{1}{2}) + \tanh(2(x-67)-\frac{1}{2})]$.

parameters of the simulation are: $\alpha = \beta = 0.14$, $m = 1 - 10^{-16}$. With this value of m the wavelength of the cnoidal wave is equal to $d \approx 75.1552$ dimensionless units, and calculations were performed on the interval of that length, $x \in [0, 75.1552]$ with a periodic boundary condition. The mesh size was taken as $N = 752$. The initial position of the wave peak was chosen at the center of chosen interval, that is $x_0 = 37.5776$. The explicit form of the initial condition in this case was $\eta(x, t = 0) = -0.0189862 + 0.368486\,\mathrm{cn}^2\left(\frac{x-x_0}{1.90221}\middle| m\right)$. Profiles of the wave are plotted at time instants $t_k = 10 \cdot k$, where $k = 0, 1, ..., 8$. Since the amplitudes of cnoidal waves are smaller than 1, the vertical shift for the sequential profiles in Figs. 5-7 is chosen to be 0.075.

In Fig. 6 we display the initially cnoidal wave moving over an extended, almost flat hump. In this simulation the value of parameters α, β, m and x interval are the same as in the previous figure. Since we consider here the motion over an uneven bottom defined by the function $h(x) = \frac{1}{2}[-\tanh(2(x-8.6)-\frac{1}{2})+\tanh(2(x-66.5552)-\frac{1}{2})]$ the evolution was calculated according to equation (1) and numerical scheme (45). Profiles of the wave are plotted at time instants $t_k = 10 \cdot k$, where $k = 0, 1, ..., 8$. Fig. 6 shows that during the wave motion over the obstacle a kind of slower wave with smaller amplitude is created following the main peak.

In Fig. 7 we present the initially cnoidal wave moving over an extended, almost flat hump. In this simulation $m = 1 - 10^{-8}$. The intial condition is given by $\eta(x, t = 0) = -0.0359497 + 0.368486\,\mathrm{cn}^2(\frac{x-x_0}{1.90221}|m)$ with $x_0 = 20.1571$. Because m is smaller than in the previous cases, the wavelength d of the cnoidal wave is also smaller, $d \approx 40.3241$. Calculations were made on the interval $x \in [0, 2d]$ with $N = 807$. Profiles of the wave are plotted at time instants $t_k = 10 \cdot k$, where $k = 0, 1, ..., 8$. Fig. 7

shows qualitatively similar features to those in Fig. 6.

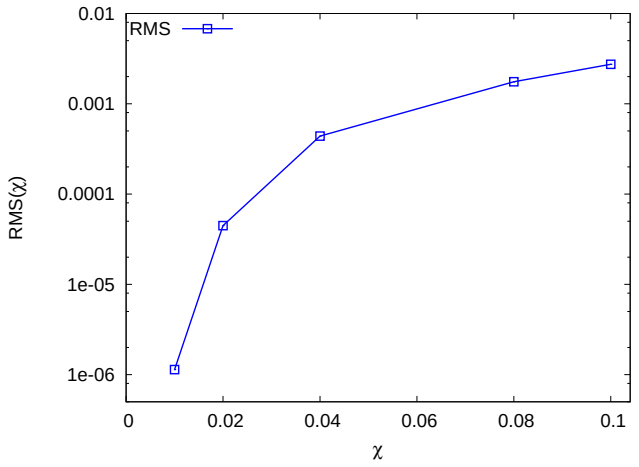

FIG. 8. Precision of numerical calculations for KdV equation in the fixed frame as a function of mesh size.

D. Precision of numerical calculations

The KdV equation (6) or (7) is unique since it possesses an infinite number of invariants, see, e.g., [8, 25]. The lowest invariant, $I_1 = \int_{-\infty}^{+\infty} \eta dx$, represents the conservation law for the mass (volume) of the liquid. The second, $I_2 = \int_{-\infty}^{+\infty} \eta^2 dx$, is related to momentum conservation, and the third, $I_3 = \int_{-\infty}^{+\infty} (\eta^3 - \frac{1}{3}\eta_x^2) dx$, is related to energy conservation. However, as pointed by [1, 2, 19], the relations between I_2 and momentum and I_3 and energy are more complex.

Approximate conservation of these invariants serves often as a test of the precision of numerical simulations. However, this is not the case for the second order KdV type equations (1) and (3). It was noted in [19] that I_1 is an invariant of equations (1) and (3) but I_2 and I_3 are not invariants. Therefore, only I_1 can be used as a test for the precision of numerical calculations of waves moving according to the second order extended KdV equations. In all the presented calculations the precision of the numerical values of I_1 was consistently high (the values $\frac{I_1(t)-I_1(0)}{I_1(0)} \leq 10^{-6}$).

Wave motion according to KdV and extended (second order) KdV equations is usually calculated in the reference frame moving with the natural velocity $c = 1$ in scaled dimensionless variables (in original variables $c = \sqrt{gh}$). The KdV and extended KdV equations for a moving reference frame are obtained by the transformation $\hat{x} = (x - t), \quad \hat{t} = t$ which removes the term η_x from the equation (3). Then the soliton velocity in the fixed frame is proportional to $1 + \frac{\alpha}{2}$ whereas in the moving frame it is proportional to $\frac{\alpha}{2}$. Therefore, for value of $\alpha = 0.1$ the distance covered by a soliton in the moving frame is $\frac{\alpha}{2}/(1 + \frac{\alpha}{2}) = \frac{1}{21}$ times shorter than the distance covered in the fixed frame for the same duration. Then, with the same number of the mesh points N the mesh size χ can be more than 20 times smaller assuring a much higher precision of calculation in the moving frame at the same operational cost. For instance [6] obtained a good precision for motion of KdV soliton with the FEM method using $N = 200$, $\chi = 0.01$ and time step $\tau = \chi$ on the interval $x \in [0, 2]$.

Precision of FEM method in the fixed frame can be tested by calculation of a root mean square (RMS) of deviations of wave profile obtained numerically from those obtained from the analytic solution. Denote by $\eta_i^{anal}(t)$ and $\eta_i^{num}(t)$ the values of the solutions at given mesh point i an time instant t, analytic and numerical, respectively. Then the RMS is expressed as

$$\mathrm{RMS}(\chi, t) = \left(\frac{1}{N} \sum_{i=1}^{N} (\eta_i^{anal}(t) - \eta_i^{num}(t))^2 \right)^{1/2} \qquad (49)$$

We checked our implementation of the FEM on the interval $x \in [0, 20]$ using several different sizes χ of the mesh and several time values. Fig. 8 displays the RMS (49) values for $t = 10$. It shows that deviations from analytic solution decrease substantialy with decreasing χ. Small χ assures a very high precision in numerical simulations, however, at the expense of large computation time. Another tests (not shown here) in which χ was fixed and RMS was calculated as a function of time showed that for $\tau = \chi^2$ RMS increases with time linerly and very slowly.

When the bottom is not flat simulations *have to be done in the fixed reference frame*. For our purposes we needed to choose the x intervals of the order of 70 or 80. Even for $\chi = 0.1$ the size of Jacobian matrices (40) reaches (4000×4000) and its inversion is time consuming. In a compromise between numerical precision and reasonable computing times we made our simulations with $\chi = 0.1$. This choice resulted in about one week of computing time for a single run on the cluster. In spite of the insufficient precision the results presented in Figs. 1-7 reproduce details of evolution known from our previous studies, obtained with the finite difference method. These details, resulting from second order terms in extended KdV (3), are seen in Fig. 1 as a wavetrain of small amplitude created behind the main one (compare with Fig. 2 in [18]). A similar wavetrain behind the main one was observed in numerical simulations by [23], see e.g. Fig. 2 therein. For waves moving with presence of bottom obstacle these secondary waves behind the main one are amplified by interaction with the bottom and new faster secondary waves appear (see, e.g., Figs. 2-4). These effects were already observed by us, see Figs. 6 and 7 in [18].

Conclusions

The main conclusions of our study can be summarized as follows.

- A weak formulation of the finite element method

(FEM) for extended KdV equation (3) can be effectively used for numerical calculations of the time evolution of both soliton and cnoidal waves when calculations are done in a moving frame.

- Since numerical calculations for equation (1) have to be performed in a fixed frame, the presented FEM method is not as effective as the FDM method used by us in previous papers because the computer time necessary for obtaining sufficiently high precision becomes impractical. On the other hand, the presented results (though not as precise as FDM ones) exhibit all secondary structures generated by higher order terms of the equations.

- First tests of numerical solutions to second order KdV type equations with a stochastic term seem to be very promising [20].

The authors would like to thank anonymous referees for several helpful suggestions and remarks that affected the article content.

[1] Ablowitz, M. and Segur, H. (1979). On the evolution of packets of water waves, Journal of Fluid Mechanics 92(4): 691–715.

[2] Ali, A. and Kalisch, H. (2014). On the formulation of mass, momentum and energy conservation in the kdv equation, Acta Applicandae Mathematicae 133(1): 113–131.

[3] Bona, J., Chen, H., Karakashian, O. and Xing, Y. (2013). Conservative, discontinuous-galerkin methods for the generalized Korteweg-de Vries equation, Mathematics of Computation 82(283): 1401–1432.

[4] Burde, G. and Sergyeyev, A. (2013). Ordering of two small parameters in the shallow water wave problem, Journal of Physics A 46: 075501.

[5] Cui, Y. and Ma, D. (2007). Numerical method satisfying the first two conservation laws for the Korteweg-de Vries equation, Journal of Computational Physics 227(1): 376–399.

[6] Debussche, A. and Printems, I. (1999). Numerical simulation of the stochastic Korteweg - de Vries equation, Physica D 134(2): 200–226.

[7] Dingemans, M. (1997). Water wave propagation over uneven bottoms, World Scientific, Singapore.

[8] Drazin, P. G. and Johnson, R. S. (1989). Solitons: An Introduc- tion, Cambridge University Press, Cambridge.

[9] Fornberg, B. and Whitham, G. B. (1978). A numerical and theoretical study of certain nonlinear wave phenomena, Philosophical Transactions A of the Royal Society 289(1361): 373–404.

[10] Goda, K. (1975). On instability of some finite difference schemes for the Korteweg – de Vries equation, Journal of the Physical Society of Japan 39: 229–236.

[11] Green, A. E. and Naghdi, P. M. (1976). A derivation of equations for wave propagation in water of variable depth, Journal of Fluid Mechanics 78(2): 237–246.

[12] Grimshaw, R. (1970). The solitary wave in water of variable depth, Journal of Fluid Mechanics 42(3): 639–656.

[13] Grimshaw, R. H. J. and Smyth, N. F. (1986). Resonant flow of a stratified fluid over topography, Journal of Fluid Mechan- ics 169: 429–464.

[14] Grimshaw, R., Pelinovsky, E. and Talipova, T. (2008). Fission of a weakly nonlinear interfacial solitary wave at a step, Geophysical and Astrophysical Fluid Dynamics 102(2): 179–194.

[15] Infeld, E. and Rowlands, G. (2000). Nonlinear Waves, Soli- tons and Chaos, 2nd edition, Cambridge University Press, Cambridge.

[16] Kamchatnov, A. M., Kuo, Y. H., Lin, T. C., Horng, T. L., Gou, S. C., Clift, R., El, G. A. and Grimshaw, R. H. J. (2012). Undular bore theory for the Gardner equation, Physical Re- view E 86: 036605.

[17] Karczewska, A., Rozmej, P. and Rutkowski, L. (2014). A new nonlinear equation in the shallow water wave problem, Physica Scripta 89(5): 054026.

[18] Karczewska, A., Rozmej, P. and Infeld, E. (2014). Shallow-water soliton dynamics beyond the Korteweg - de Vries equation, Physical Review E 90: 012907.

[19] Karczewska, A., Rozmej, P. and Infeld, E. (2015). Energy invariant for shallow water waves and the Korteweg – de Vries equation: Doubts about the invariance of energy, Physical Review E 92: 053202.

[20] Karczewska, A., Szczeciński, M., Rozmej, P. and Boguniewicz, B. (2016). Finite element method for stochastic extended KdV equations. Computational Methods in Science and Technology 22(1): 19-29.

[21] Kim, J. W., Bai, K. J., Ertekin, R. C. and Webster, W. C. (2001). A derivation of the Green-Naghdi equations for irrotational flows, Journal of Engineering Mathematics 40: 17–42.

[22] Marchant, T. and Smyth, N. (1990). The extended Korteweg – de Vries equation and the resonant flow of a fluid over topography, Journal of Fluid Mechanics 221: 263–288.

[23] Marchant, T. and Smyth, N. (1996). Soliton interaction for the extended Korteweg-de Vries equation, IMA Journal of Ap- plied Mathematics 56: 157–176.

[24] Mei, C. and Le Méhauté, B. (1966). Note on the equations of long waves over an uneven bottom, Journal of Geophysical Research 71(2): 393–400.

[25] Miura, R. M., Gardner, C. S. and Kruskal, M. D. (1968). Korteweg – de Vries equation and generalizations II. existence of conservation laws and constants of motion, Journal of Mathematical Physics 9(8): 1204–1209.

[26] Nadiga, B., Margolin, L. and Smolarkiewicz, P. (1996). Different approximations of shallow fluid flow over an obstacle, Physics of Fluids 8: 2066–2077.

[27] Nakoulima, O., Zahibo, N. Pelinovsky, E., Talipova, T. and Kurkin, A. (2005). Solitary wave dynamics in shallow water over periodic topography, Chaos 15(3): 037107.

[28] Pelinovsky, E., Choi, B., Talipova, T., Woo, S. and Kim, D. (2010). Solitary wave transformation on the underwater step: theory and numerical experiments, Applied Mathe- matics and Computation 217(4): 1704–1718.

[29] Pudjaprasetya, S. R. and van Greoesen, E. (1996). Unidirectional waves over slowly varying bottom. Part II: Quasi-homogeneous approximation of distorting waves,

Wave Motion 23: 23–38.

[30] Remoissenet, M. (1999). Waves Called Solitons: Concepts and Experiments, Springer, Berlin.

[31] Skogstad, J. and Kalisch, H. (2009). A boundary value problem for the kdv equation: comparison of finite difference and Chebyshev methods, Mathematics and Computers in Sim- ulation 80(1): 151–163.

[32] Smyth, N. F. (1987). Modulation theory solution for resonant flow over topography, Proceedings of Royal Society of London A 409(1836): 79–97.

[33] Taha, T. R. and Ablowitz, M. J. (1984). Analytical and numerical aspects of certain nonlinear evolution equations III. numerical, the Korteweg – de Vries equation, Journal of Computational Physics 55(2): 231–253.

[34] van Greoesen, E. and Pudjaprasetya, S. R. (1993). Unidirectional waves over slowly varying bottom. part I: Derivation of a KdV-type of equation, Wave Motion 18(4): 345–370.

[35] Whitham, G. B. (1974). Linear and Nonlinear Waves, Wiley, New York.

[36] Yi, N., Huang, Y. and Liu, H. (2013). A direct discontinous galerkin method for the generalized Korteweg-de Vries equation: energy conservation and boundary effect, Jour- nal of Computational Physics 242: 351–366.

[37] Yuan, J.-M., Shen, J. and Wu, J. (2008). A dual-Petrov-Galerkin method for the Kawahara-type equations, Journal of Sci- entific Computing 34: 48–63.

[38] Zabusky, N. J. and Kruskal, M. D. (1965). Interaction of 'solitons' in a collisionless plasma and the recurrence of initial states, Physical Review Letters 15(6): 240–243.